Covalently functionalized MoS_2 with dithiolenes

Ioanna K. Sideri,[a] Raul Arenal*[b, c, d] and Nikos Tagmatarchis*[a]

[a] Theoretical and Physical Chemistry Institute, National Hellenic Research Foundation, 48 Vassileos Constantinou Avenue, 11635 Athens, Greece.

[b] Laboratorio de Microscopias Avanzadas, Instituto de Nanociencia de Aragon, Universidad de Zaragoza, 50018 Zaragoza, Spain.

[c] ARAID Foundation, 50018 Zaragoza, Spain.

[d] Instituto de Ciencias de Materiales Aragon, CSIC-U. Zaragoza, 50009 Zaragoza, Spain.

ABSTRACT: Advances are required to develop functionalization routes for MoS_2, in both the metallic *1T* and semiconducting *2H* phase, that will not only enable their easier manipulation and handling in liquid media but also enhance their applicability in diverse technological fields. Herein, we report an original functionalization methodology for covalently incorporating dithiolene units at the periphery of exfoliated *1T*- and *2H*-MoS_2 sheets, by employing a bis(thiolate) salt as a ligand in a green and facile protocol. Extensive characterization of the covalently functionalized materials is presented, along with a pathway for the *à la carte* chemical manipulation of MoS_2. Markedly, the reported methodology may be applied for modifying of other transition metal dichalcogenides.

Molybdenum disulfide (MoS_2) is a 2D layered material that can be either produced via top-down exfoliation procedures from the bulk or synthesized from inorganic salts and/or organometallic species via bottom-up solvothermal routes.[1] Interestingly, MoS_2 appears with different symmetry and polymorphs, including the *2H* semiconducting and *1T* metallic phase, with the former being thermodynamically stable. Functionalization of MoS_2 has proven to be of fundamental importance towards controlling and tuning the electronic and optical properties of the material.[2] In this context, functionalized MoS_2-based nanomaterials are suitable for applications in diverse technological fields, hence, attracting enormous research interest the last few years.[3]

Although the basal plane of *2H*-MoS_2 is relatively chemically inert, functionalization routes encompassing thiol conjucation,[4, 5, 6] coordination to metal complexes,[7] diazonium radical additions[8,] and reaction with maleimides[9] were reported. An alternative route to modify semiconducting *2H*-MoS_2 is by filling S vacancies located at the edges. To this end, our team demonstrated a straightforward methodology for the covalent functionalization of *2H*-MoS_2 nanosheets by reaction with 1,2-dithiolane derivatives, which possess high binding affinity for Mo atoms.[10-16] Conversely, modification of *1T*-MoS_2 upon reactions with alkyl halides,[17, 18] aryl halides,[19] and diazonium salt electrophiles,[20, 21] were reported. Please note that in those reactions, nucleophilicity and therefore reactivity enhancement of S atoms on the basal plane due to lithium intercalation during exfoliation of MoS_2 by organolithium agents was considered. Also, it was found that *1T*-MoS_2 can electrochemically intercalate other ions as well (H^+, Na^+ and K^+) apart from Li^+.[22] Nevertheless, despite those strategies employed for modifying the basal plane and the edges of either semiconducting or metallic MoS_2, the chemistry of the material still lags behind as compared with the significant advancements witnessed on graphene during the last decade.[23] Hence, additional research effort is required to discover new functionalization routes and further develop the chemistry of MoS_2, allowing easier manipulation and processing in wet media.

Bis(thiolate) salts serve as excellent dithiolene ligands for transition metal complexes and have been studied thoroughly since their introduction in early '60s[24] due to their remarkable electrochemical and photochemical properties.[25, 26] Dithiolene chemistry has been fuelled by its multiple applications in electrochemistry,[27] biochemistry,[28] photochemistry,[29] and materials science.[30] Although dithiolenes have been extendedly studied as ligands in organometallic chemistry, their effective chemical incorporation in MoS_2 nanosheets yet awaits exploration.

Herein, we apply a novel, green and facile method for the covalent functionalization of MoS_2 employing a bis(thiolate) salt as ligand. The protocol is successfully applied in metallic *1T*-MoS_2 as well as semiconducting *2H*-MoS_2 (**Scheme 1**). Vibrational IR and Raman spectroscopy and dynamic light scattering together with microscopy imaging coupled with electron energy loss spectroscopy provide direct evidence for the chemical functionalization of the two polytype MoS_2 materials, while TGA aids to determine the organic addend loading. The route to covalently functionalize MoS_2 by attaching "custom-made" dithiolene ligands is also described and constitutes a key point not to be missed.

The MoS_2 *1T*-phase is acquired by chemical exfoliation process via Li intercalation (**1a**),[31] while conversely, chlorosulfonic acid-assisted treatment of bulk MoS_2 provides exfoliated *2H*-MoS_2 (**1b**),[32] which possesses S-vacancy sites at the edges of the basal plane. On the other hand, (*Z*)-but-2-ene-2,3-bis(thiolate) potassium salt (**2**) is synthesized via a simple three-step route.[33] Briefly, 3-chlorobutan-2-one is S_N2 substituted by *O*-isopropylxanthate salt to form *O*-isopropyl S-3-oxobutan-2-yl dithiocarbonate intermediate, which is then forced to acid-catalyzed ring closure.

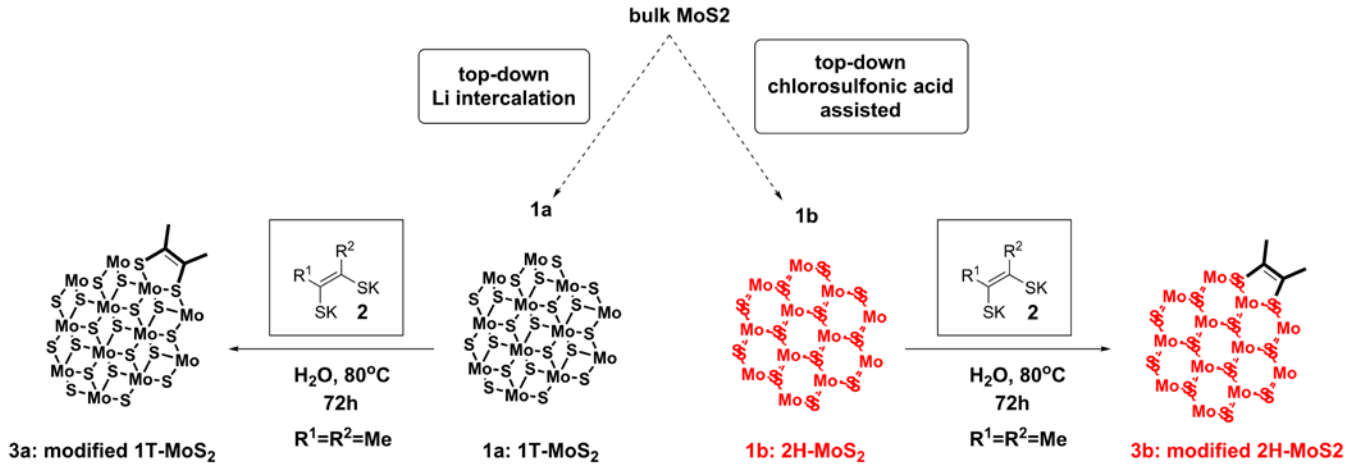

Scheme 1. Covalently functionalized *1T*- and *2H*-MoS_2 with dithiolenes.

After isolating 1,3-dithiol-2-one, subsequent KOH hydrolysis leads to (**2**) (Figure S1), according to ^{1}H NMR (Figure S2).[33] Next, an aqueous mixture of (**2**) and MoS_2 nanosheets (**1a**) and (**1b**) is thermally stirred to furnish MoS_2-modified materials (**3a**) and (**3b**), respectively, according to **Scheme 1**. The functionalized materials (**3a**) and (**3b**) are isolated by filtration, after being successively bath sonicated, filtrated over PTFE membrane (0.2 μm pore size) and extensively washed with water, methanol, DMSO and dichloromethane, to rule out the possibility of physisorption. The latter is confirmed by successive ^{1}H-NMR measurements of the filtrate until no organic compound was detected (Figure S3). Please note that the organic adduct **2**, whereas rather plain and easy to characterize for the needs of this study, can be easily modifiable as desired, e.g. bromination of the methyl group followed by a nucleophilic substitution,[34] for future studies.

Initially, electronic absorption spectroscopy reveals the metallic or semiconducting character of the starting MoS_2 materials and their modified analogues. Figure S4 illustrates the UV-Vis spectra of all four materials (**1a**, **b** and **3a**, **b**) dispersed in DMF. In the absorbance spectra of metallic (**1a**) and (**3a**), a broad absorption band at 600-700 nm is depicted along with a characteristic band at 420 nm (Figure S4a).[35] On the other hand, *2H*-MoS_2 (**1b**) and (**3b**) are distinguished by their characteristic A and B excitonic transitions at 690 and 630 nm, respectively, while C and D excitonic peaks appear at 470 and 400 nm, respectively (Figure S4b).[36]

Next, Raman spectroscopy measurements (λ_{exc} 633 nm) are conducted. The Raman spectrum of (**3a**) reveals all characteristic modes of MoS_2 in the range of 300-500 cm^{-1}. In detail, in-plane transition E^1_{2g} at 375 cm^{-1}, out-of-plane transition A_{1g} at 405 cm^{-1} and S-vacancies-related 2LA(M)[37] vibration at 450 cm^{-1} are depicted (Figure 1). Particularly the intensity of the 2LA(M) mode is decreased as compared with that of (**1a**), which is an essential hint of lattice healing. Characteristic J_1, J_2 and J_3 modes of *1T*-MoS_2 polytype at 150, 220, and 325 cm^{-1} respectively are also present, confirming the predominantly metallic character of (**1a**) and (**3a**). On the other hand, while *2H*-MoS_2 characteristic E^1_{2g}, A_{1g} and 2LA(M) modes are present and way defined in the Raman spectra of (**1b**) and (**3b**) (Figure 2), the absence of J_1, J_2 and J_3 associated with the phonon modes of *1T*-MoS_2 advocates for a *2H*-phase character, which is preserved upon dithiolenes functionalization. Moreover, focusing on the 2LA(M) mode of (**3b**), there is a considerable decrease in intensity compared to that of (**1b**), therefore again a strong indication of functionalization is given. Complementary Raman mapping assays highlight the increased $I_{A1g}/I_{2LA(M)}$ intensity ratio of functionalized materials (**3a**) and (**3b**) compared to that of starting (**1a**) and (**1b**), supporting this allegation (Figure 1 and Figure 2).

Figure 1. Top: Raman spectra of exfoliated *1T*-MoS_2 (**1a**-black) and functionalized *1T*-MoS_2 (**3a**-red) (normalized at the A_{1g} mode). Bottom-left: 2D Raman mapping of the $I_{A1g}/I_{2LA(M)}$ intensity ratio of a 20μm x 20μm area for exfoliated *1T*-MoS_2 (**1a**). Bottom-right: 2D Raman mapping of the $I_{A1g}/I_{2LA(M)}$ intensity ratio of a 20μm x 20μm area for functionalized *1T*-MoS_2 (**3a**). All measurements were conducted at λ_{exc} 633 nm.

Figure 2. Raman spectra of exfoliated *2H*-MoS_2 (**1b**-black) and functionalized *2H*-MoS_2 (**3b**-red) (normalized at the A_{1g} mode). Bottom-left: 2D Raman mapping of the $I_{A1g}/I_{2LA(M)}$ intensity ratio of a 20μm x 20μm area for exfoliated *2H*-MoS_2 **1b**. Bottom-right: 2D Raman mapping of the $I_{A1g}/I_{2LA(M)}$ intensity ratio of a 20μm x 20μm area for functionalized *2H*-MoS_2 (**3b**). All measurements were conducted at λ_{exc} 633 nm.

Regarding ATR-IR spectroscopy, while MoS_2 (**1a**) and (**1b**) do not bare any functional groups and therefore characteristic vibrations are absent, the spectrum of organic bis(thiolate) salt (**2**) reveals the C-H stretching vibration bands at 2976 cm^{-1}, 2925 cm^{-1} and 2825 cm^{-1} as well as C=C and C-S stretching bands at around 1600 and 702 cm^{-1}, respectively (Figure S5). These identifying signals are also present in the modified materials (**3a**) and (**3b**), as illustrated in Figure 3. Based on this strong proof for the presence of dithiolenes in (**3a**) and (**3b**), along with the S-vacancies-related decreased 2LA(M) mode in the modified MoS_2 materials and the work-up procedure employed to remove any physisorbed organic species, as previously described, we conclude that the dithiolene moieties are covalently attached to MoS_2.

In an attempt to gain further insight into the structure of the novel materials synthesized, we subjected the samples to electron transmission microscopy (TEM) imaging. We analyzed exfoliated and functionalized *1T*-MoS_2 and *2H*-MoS_2 via high-resolution scanning TEM (HRSTEM) imaging and spatially-resolved electron energy loss spectroscopy (SR-EELS). HRSTEM imaging is one of the most appropriate techniques to investigate the structural phase, i.e. *1T* or *2H*, of these MoS_2 nanosheets,[32, 38, 39] while SR-EELS is an essential technique for the chemical investigation at the local state.[13, 16, 40-42] Four different high-angle annular dark-field HRSTEM micrographs, corresponding to exfoliated (**1a**) and functionalized (**3a**) *1T*-MoS_2, and exfoliated (**1b**) and functionalized (**3b**) *2H*-MoS_2 are shown at Figure 4a and b, respectively. The images confirm that the original phase of exfoliated (**1a**) and (**1b**) has been preserved after the functionalization on the corresponding dithiolene-modified (**3a**) and (**3b**) materials, respectively. By observing numerous flakes, the size of MoS_2 sheets is in the range of 100-1000 nm, as evidenced by the corresponding low magnification STEM images (Figure S6). These findings have been corroborated by SR-EELLS STEM analyses performed on (**3a**) and (**3b**) and compared with that of (**1a**) and (**1b**), respectively (Figure 5). The S-$L_{2,3}$, Mo-$M_{4,5}$, C-K and Mo-$M_{2,3}$ edges are evident in the spectra of functionalized (**3a**) and (**3b**). However, the C-K signal, characteristic of the added dithiolene units, is absent in the corresponding EEL spectra of exfoliated (**1a**) and (**1b**). Hence, based on these EELS analyses the presence of dithiolene moieties is confirmed in the functionalized *2H*-MoS_2 and *1T*-MoS_2 flakes.

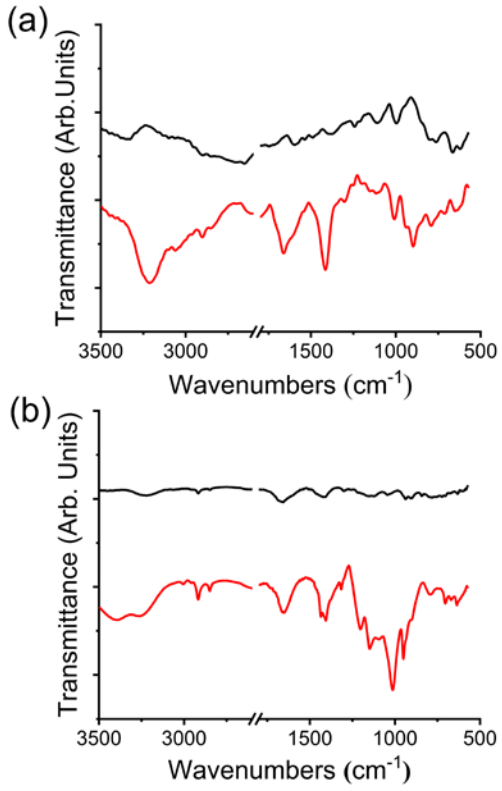

Figure 3. ATR-IR spectra of a) exfoliated *1T*-MoS_2 (**1a**-black) and functionalized *1T*-MoS_2 (**3a**-red) and b) exfoliated *2H*-MoS_2 (**1b**-black) and functionalized *2H*-MoS_2 (**3b**-red).

Complementary, the size of exfoliated (**1a**) and (**1b**) and their functionalized analogues (**3a**) and (**3b**), respectively, is estimated by dynamic light scattering (DLS) assays. The apparent hydrodynamic radius (R_h) of (**1a**) is found to be 163 nm, whereas the R_h of (**1b**) is 271 nm. Conversely, the R_h of functionalized (**3a**) and (**3b**) is 305 and 411 nm, respectively. The upsize of functionalized MoS_2 by approximately 140 nm, as compared to exfoliated material, is rationalized by considering aggregation effects as well as the functionalization and incorporation of the hydrophobic dithiolene moieties at the periphery of the nanosheets. The deviation in size observed between HRSTEM and DLS is not actually invalid. DLS provides the apparent average hydrodynamic radius based on size distribution in an aqueous dispersion, where nanoaggregates may form, while in HRSTEM the samples are imaged in solid form.

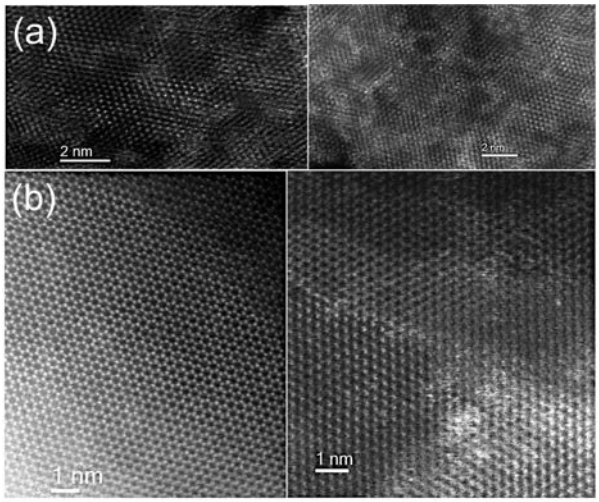

Figure 4. HRSTEM-HAADF micrographs of a) exfoliated *1T*-MoS_2 (**1a**-left) and functionalized *1T*-MoS_2 (**3a**-right), and b) exfoliated *2H*-MoS_2 (**1b**-left) and functionalized *2H*-MoS_2 (**3b**-right).

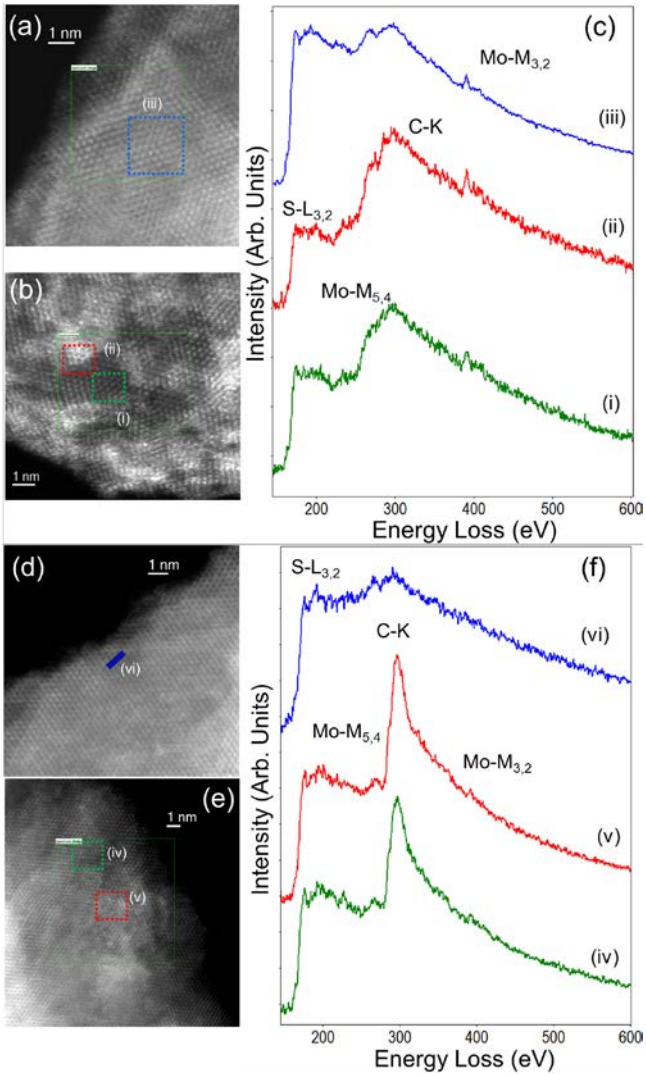

Figure 5. (a, b) HAADF-STEM images of exfoliated *1T*-MoS_2 (**1a**) and functionalized *1T*-MoS_2 (**3a**), respectively. EELS spectra-image (SPIM) have been recorded in the green marked areas highlighted in these images. (c) Three EEL spectra corresponding to the sum of 56 (64, for SPIM of Fig. 5a) spectra collected in each of the three highlighted areas (marked (i), (ii) and (iii) of these SPIM, see Fig. 5a and b HAADF micrographs). (d and e) HAADF-STEM images of exfoliated *2H*-MoS_2 (**1b**) and functionalized *2H*-MoS_2 (**3b**), respectively. An EELS spectrum-line (SPLI) and an EELS SPIM have been collected in the blue and green marked areas highlighted in these images. (f) Three EEL spectra corresponding to the sum of 5 (36, for SPIM of Fig. 5d) spectra recorded in each of the three highlighted areas (marked (i), (ii) and (iii) of these SPLI and SPIM, see Fig. 5 c and d HAADF micrographs).

Thermogravimetric analysis along with further implication of successful incorporation of (**2**) on MoS_2 lattice reveals also the degree of functionalization for each material. While (**1a**) exhibits a mass loss of 2.7% up to 500°C, mainly due to the intercalation conditions that affect the structural homogeneity of MoS_2,[20] (**3a**) shows a 6.5% mass loss, therefore the 3.8% mass loss is attributed to the decomposition of the organic addend (Figure 6a). On the other hand, semiconducting *2H*-MoS_2 (**1b**) is rather thermally stable up to 500 °C, whereas functionalized material (**3b**) shows a minor but 2.3% mass loss up to that temperature (Figure 6b), indicating that S vacancies at the edges are occupied by bis(thiolate) salt (**2**).

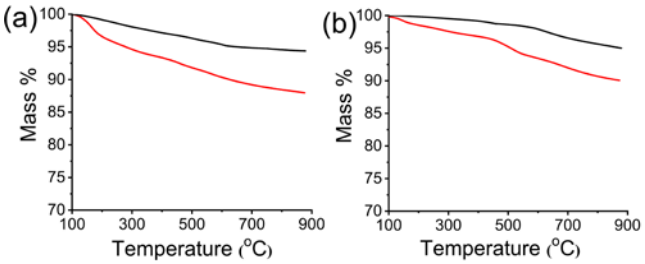

Figure 6. TGA graphs of exfoliated a) *1T*-MoS_2 (**1a**-black) and functionalized material (**3a**- red), and b) exfoliated *2H*-MoS_2 (**1b**-black) and functionalized material (**3b**-red).

In conclusion, we present a straightforward and eco-friendly protocol for the covalent functionalization of *1T*-MoS_2 and *2H*-MoS_2 utilizing water as solvent and mild reaction conditions. In particular, we showcase that both phases of MoS_2 can be covalently functionalized with a simple bis(thiolate) salt, therefore incorporating dithiolene chemistry and its outstanding applications in materials science. Our study provides the research community with the tools to modify MoS_2 as desired by designing "custom-made" dithiolene reagents bearing active moieties.

ASSOCIATED CONTENT

Supporting Information. Experimental procedures, synthetic route and characterization data. This material is available free of charge via the Internet at http://pubs.acs.org.

AUTHOR INFORMATION

Corresponding Authors

*E-mail: tagmatar@eie.gr
*E-mail: arenal@unizar.es

Author Contributions

The manuscript was written through contributions of all authors. All authors have given approval to the final version of the manuscript.

Notes

The authors declare no competing financial interest.

ACKNOWLEDGMENTS

Partial support of this work by the project "Advanced Materials and Devices" (MIS 5002409) which is implemented under the "Action for the Strategic Development on the Research and Technological Sector" funded by the Operational Program "Competitiveness, Entrepreneurship and Innovation" (NSRF 2014-2020) and co-financed by Greece and the European Union (European Regional Development Fund) is acknowledged. R.A. gratefully acknowledges the support from the Spanish Ministerio de Economia y Competitividad (MAT2016-79776-P), from the Government of Aragon and the European Social Fund under the project "Construyendo Europa desde Aragon" 2014-2020 (grant number E13_17R) and from EU H2020 program "ESTEEM3" (823717) and "Graphene Flagship" (785219 and 881603).

REFERENCES

(1) Wang, H.; Li, C.; Fang, P.; Zhang, Z.; Zhang, J. Z. Synthesis, Properties, and Optoelectronic Applications of Two-Dimensional MoS_2 and MoS_2-based Heterostructures. *Chem. Soc. Rev*. **2018**, *47*, 6101-6127.

(2) Stergiou A.; Tagmatarchis, N. Molecular Functionalization of Two-Dimensional MoS_2 Nanosheets. *Chem. Eur. J*. **2018**, *24*, 18246-18257.

(3) Anichini, C.; Czepa, W.; Pakulski, D.; Aliprandi, A.; Ciesielski, A.; Samorì P. Chemical Sensing with 2D Materials. *Chem. Soc. Rev*. **2018**, *47*, 4860-4908.

(4) Chou, S. S.; De, M.; Kim, J., Byun, S.; Dykstra, C.; Yu, J.; Huang, J.; Dravid, V. P. Ligand Vonjucation of Chemically Exfoliated MoS_2. *J. Am. Chem. Soc.* **2013**, *135*, 4584-4587.

(5) Ding, Q.; Czech, K. J.; Zhao, Y.; Zhai, J.; Hamers, R. J.; Wright, J. C.; Jin, S. Basal-Plane Ligand Functionalization on Semiconducting 2H-MoS_2 Monolayers. *ACS Appl. Mater. Interfaces* **2017**, *9*, 12734-12742.

(6) Karunakaran, S.; Pandit, S.; Basu, B.; De, M. Simultaneous Exfoliation and Functionalization of 2H-MoS_2 by Thiolated Surfactants: Applications in Enhanced Antibacterial Activity. *J. Am. Chem. Soc*. **2018**, *140*, 12634-12644.

(7) Backes, C.; Berner, N. C.; Chen, Xi.; Lafargue, P.; LaPlace, P.; Freeley, M.; Duesberg, G. S.; Coleman, J. N.; McDonald, A.R.; Functionalization of Liquid-Exfoliated Two-Dimensional 2H-MoS_2. *Angew. Chem. Int. Ed*. **2015**, *54*, 2638-2642.

(8) Chu, X. S.; Yousaf, A.; Li, D. O.; Tang, A. A.; Debnath, A.; Ma, D.; Green, A. A.; Santos, E. J. G.; Wang, Q. H. Direct Covalent Chemical Functionalization of Unmodified Two-Dimensional Molybdenum Disulfide. *Chem. Mater*. **2018**, *30*, 2112-2128.

(9) Vera-Hidalgo, M.; Giovanelli, E.; Navío, C.; Pérez, E. M. Mild Covalent Functionalization of Transition Metal Dichalcogenides with Maleimides: A "Click" Reaction for 2H-MoS_2 and WS_2. *J. Am. Chem. Soc*. **2019**, *141*, 3767-3771.

(10) Canton-Vitoria, R.; Sayed-Ahmad-Baraza, Y.; Pelaez-Fernandez, M.; Arenal, R.; Bittencourt, C.; Ewels, C. P.; Tagmatarchis, N. Functionalization of MoS_2 With 1,2-Dithiolanes: Toward Donor-Acceptor Nanohybrids for Energy Conversion. *NPJ2D Mater. Appl*. **2017**, *1*, 13.

(11) Canton-Vitoria, R., Stangel, C.; Tagmatarchis, N. Electrostatic Association of Ammonium-Functionalized Layered-Transition-Metal Dichalcogenides with an Anionic Porphyrin. *ACS Appl. Mater. Interfaces* **2018**, *10*, 23476-23480.

(12) Canton-Vitoria, R.; Vallan, L.; Urriolabeitia, E.; Benito, A. M.; Maser W. K.; Tagmatarchis, N. Electronic Interactions in Illuminated Carbon Dot/MoS_2 Ensembles and Electrocatalytic Activity towards Hydrogen Evolution. *Chem. Eur. J*. **2018**, *24*, 10468-10474.

(13) Vallan, L.; Canton-Vitoria, R.; Gobeze, H. B.; Jang, Y.; Arenal, R.; Benito, A. M.; Maser, W. K.; D'Souza. F.; Tagmatarchis, N. Interfacing Transition Metal Dichalcogenides with Carbon Nanodots for Managing Photoinduced Energy and Charge-Transfer Processes. *J. Am. Chem. Soc*. **2018**, *140*, 13488-13496.

(14) Canton-Vitoria, R.; Gobeze, H. B.; Blas-Ferrando, V. M.; Ortiz, J.; Jang, Y.; Fernández-Lázaro, F.; Sastre-Santos, Á.; Nakanishi, Y.; Shinohara, H.; D'Souza, F.; Tagmatarchis, N. Excited-State Charge Transfer in Covalently Functionalized MoS_2 with a Zinc Phthalocyanine Donor-Acceptor Hybrid. *Angew. Chem. Int. Ed*. **2019**, *58*, 5712-5717.

(15) Canton-Vitoria, R.; Istif, E.; Hernández-Ferrer, J.; E. Urriolabeitía, A.; Benito, M.; Maser, W. K.; Tagmatarchis, N. Integrating Water-Soluble Polythiophene with Transition-Metal Dichalcogenides for Managing Photoinduced Processes. *ACS Appl. Mater. Interfaces* **2019**, *11*, 5947-5956.

(16) Canton-Vitoria, R.; Scharl, T.; Stergiou, A.; Cadranel, A.; Arenal, R.; Guldi, D. M.; Tagmatarchis, N. Ping-Pong Intercomponent Energy Transfer in Covalently Linked Porphyrin–MoS_2 Architectures. *Angew. Chem. Int. Ed*. **2020**, *59*, 3976-3981.

(17) Voiry, D.; Goswami, A.; Kappera, R.; de Carvalho, C.; Silva, C.; Kaplan, D.; Fujita, T.; Chen, M.; Asefa, T.; Chhowalla, M. Covalent Functionalization of Monolayered Transition Metal Dichalcogenides by Phase Engineering. *Nat. Chem*. **2015**, *7*, 45-49.

(18) Yan, E. X.; Caban-Acevedo, M.; Papadantonakis, K. M.; Brunschwig, B. S.; Lewis, N. S. Reductant-Activated, High-Coverage, Covalent Functionalization of 1T′-MoS_2. *ACS Materials Lett.* **2020**, *2*, 133-139.

(19) Vishnoi, P.; Sampath, A.; Waghmare, U. V.; Rao, C. N. R. Covalent Functionalization of Nanosheets of MoS_2 and $MoSe_2$ by Substituted Benzenes and Other Organic Molecules. *Chem. Eur. J*. **2017**, *23*, 886-895.

(20) Knirsch, K. C.; Berner, N. C.; Nerl, H. C.; Cucinotta, C. S.; Gholamvand, Z.; McEvoy, N.; Wang, Z.; Abramovic, I.; Vecera, P.; Halik, M.; Sanvito, S.; Duesberg, G. S.; Nicolosi, V.; Hauke, F.; Hirsch, A.; Coleman, J. N.; Backes, C. Basal-Plane Functionalization of Chemically Exfoliated Molybdenum Disulfide by Diazonium Salts. *ACS Nano* **2015**, *9*, 6018-6030.

(21) Benson, E. E.; Zhang, H.; Schuman, S. A.; Nanayakkara, S. U.; Bronstein, N. D.; Ferrere, S.; Blackburn, J. L.; Miller, E. M. Balancing the Hydrogen Evolution Reaction, Surface Energetics, and Stability of Metallic MoS_2 Nanosheets via Covalent Functionalization. *J. Am. Chem. Soc*. **2018**, 140, 441-450.

(22) Acerce, M.; Voiry, D.; Chhowalla, M. Metallic 1T Phase MoS_2 nanosheets as supercapacitor electrode materials. *Nature Nanotech.* **2015**, *10*, 313-318.

(23) Gong, X.; Liu, G.; Li, Y.; Yau, D.; Yu, W.; Teoh, W. Y. Functionalized-Graphene Composites: Fabrication and Applications in Sustainable Energy and Environment. *Chem. Mater*. **2016**, *28*, 8082-8118.

(24) Schrauzer, G. N.; Mayweg, V. Reaction of Diphenylacetylene with Nickel Sulfides. *J. Am. Chem. Soc*. **1962**, *84*, 3221-3221.

(25) Stiefel, E. I.; Karlin, K. D. Dithiolene Chemistry: Synthesis, Properties, and Applications, Progress in Inorganic Chemistry **2003**, 52, 1-752.

(26) Kato, R. Conducting Metal Dithiolene Complexes: Structural and Electronic Properties. *Chem. Rev*. **2004**, *104*, 5319-5346.

(27) Downes, C. A.; Marinescu, S. C. Efficient Electrochemical and Photoelectrochemical H2 Production from Water by a Cobalt Dithiolene One-Dimensional Metal-Organic Surface. *J. Am. Chem. Soc*. **2015**, *137*, 13740-13743.

(28) Ahmadi, M.; Fischer, C.; Ghosh, A. C.; Schulzke, C. An Asymmetrically Substituted Aliphatic Bis-Dithiolene Mono-Oxido Molybdenum(IV) Complex With Ester and Alcohol Functions as Structural and Functional Active Site Model of Molybdoenzymes. *Front. Chem*. **2019**, 486-500.

(29) McNamara, W. R.; Han, Z.; Yin, C.-J. M.; Brennessel, W. W.; Holland, P. L.; Eisenberg, R. Cobalt-Dithiolene Complexes for the Photocatalytic and Electrocatalytic Reduction of Protons in Aqueous Solutions. *PNAS* **2012**, *109*, 15594-15599.
(30) Clough, A. J.; Skelton, J. M.; Downes, C. A.; de la Rosa, A. A.; Yoo, J. W.; Walsh, A.; Melot, B. C.; Marinescu, S. C. Metallic Conductivity in a Two-Dimensional Cobalt Dithiolene Metal–Organic Framework. *J. Am. Chem. Soc.* **2017**, *139*, 10863-10867.
(31) Nicolosi, V.; Chhowalla, M.; Kanatzidis, M. G.; Strano M. S.; Coleman, J. N. Liquid Exfoliation of Layered Materials. *Science* **2013**, *340*, 1226419.
(32) Pagona, G.; Bittencourt, C.; Arenal R.; Tagmatarchis, N. Exfoliated Semiconducting Pure 2H-MoS_2 and 2H-WS_2 Assisted by Chlorosulfonic Acid, *Chem. Commun*. **2015**, *51*, 12950-12953.
(33) Ghosh, A. C.; Reinhardt, J. K.; Kindermann M. K.; Schulzke, C. The Ring Opening Reaction of 1,3-Dithiol-2-one Systems is Fully Reversible. *Chem. Commun*. **2014**, *50*, 10102-10104.
(34) Crivillers, N.; Oxtoby, N. S.; Mas-Torrent, M.; Veciana, J.; Rovira C. Improved Synthesis of Dithiophene-Tetrathiafulvalene. *Synthesis* **2007**, *11*, 1621-1623.
(35) Eda, G.; Yamaguchi, H.; Voiry, D.; Fujita, T.; Chen, M.; Chhowalla M. Photoluminescence from Chemically Exfoliated MoS_2. *Nano Lett.* **2011**, *11*, 5111-5116.
(36) Nguyen, E. P.; Carey, B. J.; Daeneke, T.; Ou, J. Z.; Latham, K.; Zhuiykov, S.; Kalantar-zadeh, K. Investigation of Two-Solvent Grinding-Assisted Liquid Phase Exfoliation of Layered MoS_2. *Chem. Mater*. **2015**, *27*, 53-59.
(37) Bae, S.; Sugiyama, N.; Matsuo, T.; Raebiger, H.; Shudo, K.-i.; Ohno, K. Defect-Induced Vibration Modes of Ar^+-Irradiated MoS_2. *Phys. Rev. Appl*. **2017**, *7*, 024001.
(38) Dubey, S.; Lisi, S.; Nayak, G.; Herziger, F.; N'Guyen, V. D.; Le Quang, T.; Cherkez, V.; González, C.; Dappe, Y.; Watanabe, K.; Taniguchi, T.; Magaud, L.; Mallet, P.; Veuillen, J.Y.; Arenal, R.; Marty, L.; Renard, J.; Bendiab, N.; Coraux, J.; Bouchiat, V. Weakly Bound, Charged, and Free Excitons in Single-Layer MoS2 in Presence of Defects, Strain, and Charged Impurities. *ACS Nano* **2017**, *11*, 11206-11216.
(39) Backes, C.; Abdelkader, A. M.; Alonso, C.; Andrieux, A.; Arenal, R. Production and Processing of Graphene and Related Materials. *2D Mat.* **2020**, *7*, 022001.
(40) Arenal, R.; de la Peña, F.; Stephan, O.; Walls, M.; Tence, M.; Loiseau, A.; Colliex, C. Extending the Analysis of EELS Spectrum-Imaging Data, from Elemental to Bond Mapping in Complex Nanostructures. *Ultramicroscopy* **2008**, *109*, 32-38.
(41) Arenal, R.; March, K.; Ewels, C. P.; Rocquefelte, X.; Kociak, M.; Loiseau, A.; Stephan, O. Atomic Configuration of Nitogen-Doped Single-Walled Carbon Nanotubes. *Nano Lett*. **2014**, *14*, 5509-5516.
(42) Ernst, F.; Gao, Z.; Arenal, R.; Heek, T.; Setaro, A.; Fernandez-Pacheco, R.; Haag, R.; Cognet, L.; Reich, S. Noncovalent Stable Functionalization Makes Carbon Nanotubes Hydrophilic and Biocompatible. *J. Phys. Chem. C* **2017**, *121*, 18887-18891.

ToC

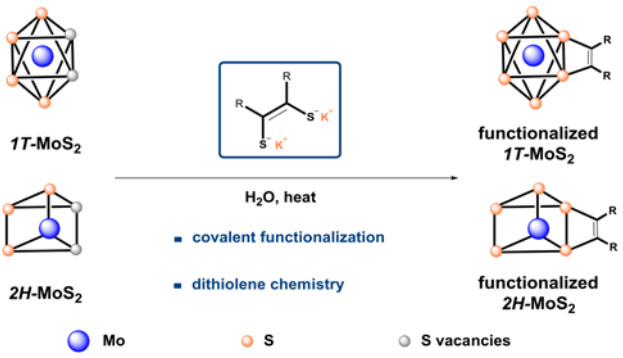
1T-MoS2
2H-MoS2
H2O, heat
covalent functionalization
dithiolene chemistry
functionalized 1T-MoS2
functionalized 2H-MoS2
Mo
S
S vacancies